

## Expressivity of Holt-Oram Syndrome Is Not Predicted by *TBX5* Genotype

Anna-Marie E. Brassington,<sup>1,\*</sup> Sandy S. Sung,<sup>1,\*</sup> Reha M. Toydemir,<sup>1</sup> Trung Le,<sup>1</sup>  
Amy D. Roeder,<sup>1</sup> Ann E. Rutherford,<sup>1</sup> Frank G. Whitby,<sup>2</sup> Lynn B. Jorde,<sup>1</sup>  
and Michael J. Bamshad<sup>1,3,4</sup>

Departments of <sup>1</sup>Human Genetics, <sup>2</sup>Biochemistry, and <sup>3</sup>Pediatrics, University of Utah Health Sciences Center, and <sup>4</sup>Shriners Hospitals for Children, Intermountain Unit, Salt Lake City

Mutations in *TBX5*, a T-box-containing transcription factor, cause cardiac and limb malformations in individuals with Holt-Oram syndrome (HOS). Mutations that result in haploinsufficiency of *TBX5* are purported to cause cardiac and limb defects of similar severity, whereas missense mutations, depending on their location in the T box, are thought to cause either more severe heart or more severe limb abnormalities. These inferences are, however, based on the analysis of a relatively small number of independent cases of HOS. To better understand the relationship between mutations in *TBX5* and the variable expressivity of HOS, we screened the coding and noncoding regions of *TBX5* and *SALL4* for mutations in 55 probands with HOS. Seventeen mutations, including six missense mutations in *TBX5* and two mutations in *SALL4*, were found in 19 kindreds with HOS. Fewer than 50% of individuals with nonsense or frameshift mutations in *TBX5* had heart and limb defects of similar severity, and only 2 of 20 individuals had heart or limb malformations of the severity predicted by the location of their mutations in the T box. These results suggest that neither the type of mutation in *TBX5* nor the location of a mutation in the T box is predictive of the expressivity of malformations in individuals with HOS.

### Introduction

Congenital heart defects are the most frequent birth defect observed in humans and the most common cause of death in infancy (Guyer et al. 1998). Although the etiology of most heart defects is unknown, many of them are thought to have a genetic basis (Burn et al. 1998; Loffredo 2000). Consequently, understanding the molecular basis of heart malformations has been a major focus of biomedical research over the past decade. To this end, investigators have sought to gain insights about the genetic etiology of cardiac malformations by identifying genes underlying rare, Mendelian syndromes in which heart defects are a major feature. A prototypical example of such a condition is Holt-Oram syndrome (HOS [MIM 142900]), a disorder characterized by limb as well as heart malformations. Most individuals with HOS have either a secundum atrial septal defect (ASD) or a ventricular septal defect (VSD), although many other cardiac malformations have been reported, ranging from mitral valve prolapse to hypoplastic left heart (Newbury-Ecob et al. 1996; Sletten and Pierpont 1996; Bruneau et al. 1999).

Received March 10, 2003; accepted for publication April 10, 2003; electronically published June 3, 2003.

Address for correspondence and reprints: Dr. Mike Bamshad, Eccles Institute of Human Genetics, 15 North 2030 East, University of Utah, Salt Lake City, UT 84112. E-mail: mike@genetics.utah.edu

\* The first two authors contributed equally to this work.

© 2003 by The American Society of Human Genetics. All rights reserved.  
0002-9297/2003/7301-0008\$15.00

In 1997, HOS was discovered to be caused by mutations in *TBX5* (Basson et al. 1997; Li et al. 1997), one of a family of transcription factors, called “T-box” genes, that have been associated with a variety of malformations (Bamshad et al. 1997; Braybrook et al. 2001; Merscher et al. 2001). Most of the mutations in *TBX5* were predicted to encode, if translated, a truncated protein that lacked a functional DNA-binding domain. These mutations often were found in individuals in whom the heart and limbs were affected with similar severity. This led to the inference that most cases of HOS were caused by haploinsufficiency of *TBX5*, which, in turn, disrupted both limb and heart development to a similar extent.

In several kindreds with HOS, individuals who had heart and limb defects of disparate severity were found to have missense mutations, suggesting that, in some cases, HOS might be caused by a dominant-negative mechanism (Basson et al. 1994, 1997). This observation led to the proposal that missense mutations predicted to disturb different regions of the T box might be associated with organ-specific defects (Basson et al. 1999). Specifically, an amino acid substitution in the N-terminal end of the T box (i.e., Gly80Arg), predicted to affect *TBX5* binding to the major groove of target DNA, was found to cause severe heart malformations but relatively mild limb defects in a single, large kindred. Alternatively, two amino acid substitutions in the C-terminal end of the T box (Arg237Gln and Arg237Trp), which were predicted to perturb *TBX5* binding to the

minor groove of target DNA, were found to cause mild cardiac abnormalities but severe limb defects.

These findings suggested that *TBX5* genotypes might be predictive of the expressivity of HOS, a compelling interpretation for several reasons. First, it implied that different regions of the T box might impart functional specificity to *TBX5* (Schneider and Schwartz 1999). This inference was reinforced by transactivation studies that demonstrated that *Tbx5* mutants with a Gly80Arg substitution associated with severe heart malformations failed to activate atrial natriuretic factor (*ANF*), whereas *Tbx5* mutants with an Arg237Gln substitution activated *ANF* to a level similar to wild-type *Tbx5* (Hiroi et al. 2001). Second, it suggested that genetic counseling of individuals with HOS might be facilitated by making inferences about anticipatory guidance, based on *TBX5* genotypes. Third, it increased the plausibility that some mutations in the T box of *TBX5* might cause isolated heart malformations, particularly ASDs or VSDs.

For several reasons, it is not clear that *TBX5* genotypes are predictive of the expressivity or the extent of pleiotropy in HOS. First, all of the study subjects with HOS caused by a Gly80Arg substitution reported by Basson et al. (1999) were members of the same kindred, and some of the individuals with Arg237Gln or Arg237Trp were related to one another. Thus, the suggested genotype-phenotype correlation was based on only a few independent cases. Second, only several other missense mutations in the T box of *TBX5* have been reported to date, and no study has compared *TBX5* genotypes to HOS phenotypes in a large cohort of cases. Third, more recent studies of the DNA-binding characteristics of mutant *Tbx5* proteins have demonstrated that *Tbx5* mutants with either the Gly80Arg or the Arg237Gln substitution failed to bind to a preferred target DNA sequence identified via an in vitro selection procedure (Ghosh et al. 2001; Fan et al. 2003). Therefore, if neither mutant binds the target DNA of *TBX5*, it is unclear how missense mutations in different regions of the T box of *TBX5* might cause heart and limb defects of disparate severity.

To further explore the relationship between *TBX5* genotypes and HOS phenotypes, we screened the coding and noncoding regions of *TBX5* for mutations in 55 probands with HOS—to our knowledge the largest collection of patients with HOS studied to date. Fourteen different mutations, including six missense mutations, were found in 17 kindreds in which affected individuals spanned the spectrum of HOS phenotypes. We found no evidence that either the type of mutation or the location of a mutation in *TBX5* was predictive of the severity of limb or heart malformations in a patient with HOS. Only two mutations in *TBX5* were found in probands with phenotypes atypical of HOS (i.e., individuals with heart and limb defects accompanied by physi-

cal findings—e.g., *situs inversus*—not commonly found in patients with HOS), and novel mutations in *SALL4* were found in an additional two of these atypical cases.

## Material and Methods

### Clinical Status

All studies were performed with the approval of the institutional review board of the University of Utah and the general counsel of the Shriners Hospitals for Children. After obtaining informed consent, most living members of each kindred were evaluated by review of their medical history, physical examination, radiographs of the upper limbs, electrocardiogram, and echocardiogram. Heart and limb malformations were classified as mild or severe according to criteria established elsewhere (Basson et al. 1999). In brief, individuals with unilateral or bilateral hypoplasia or aplasia of both the humerus and radius were categorized as having severe limb defects; otherwise, affected individuals were considered to have mild limb defects. Individuals with multiple septation defects (e.g., an ASD and a VSD), a single septal defect plus another cardiac anomaly, or complex congenital heart disease were categorized as having severe heart defects. Individuals with a single septal defect or only an electrocardiographic abnormality were categorized as having a mild heart defect. All subjects included in the analysis had normal karyotypes.

### Mutation Analysis

Genomic DNA was extracted from peripheral lymphocytes through use of standard techniques. DNA sequences were amplified using 25 ng genomic DNA as a template in 1 × buffer (1.5 mM MgCl<sub>2</sub>; 10 mM Tris.Cl, pH 8.3; 20% Q solution [Qiagen]), 0.5 U QIAGEN hotstar *Taq* polymerase, and 10 pmol of each primer. Samples were cycled 30 times in an MJ Research DNA Engine Tetrad, using a standard three-step PCR profile with an initial denaturing step at 94°C for 15 min and a final extension step at 72°C for 10 min. Annealing temperatures and primer sequences can be found in table A (online only). PCR products were purified by size exclusion or gel extraction using a QIAquick column. Purified PCR products were sequenced using ABI BigDye terminator cycle sequencing version 2.0 reagent. Sequenced products were loaded on an ABI 377 automated sequencer and were analyzed by Sequencing Analysis 3.4.1 and SEQUENCHER 4.1 software (Genecodes). The forward and reverse strand of exons 1–9 of *TBX5*, including the flanking splice-recognition sequences, were analyzed. Complete sequence data were available for 49 of 55 probands.

The presence of each missense and nonsense mutation was confirmed in each affected individual by either re-

**Table 1**

**Phenotype, Severity Score, and *TBX5*/*SALL4* Genotype in Individuals Diagnosed with HOS**

GENE MUTATED, KINDRED, AND PATIENT	PHENOTYPE <sup>a</sup>					MUTATION	SEVERITY OF PHENOTYPE <sup>b</sup>	
	Heart	Hand	Arm	Other	Heart		Limb	
<b><i>TBX5</i>:</b>								
K1:								
II-2	ASD	Absent digit (B1)	Absent radius (B)			456delC	M	S
K2:								
I-1	Normal echo	Absent digit (B1), hypoplastic digit (B2-5)	Hypoplastic radius, ulna, humerus (L)	Hypoplastic chest wall, abnormal shoulder girdle		100delG	M	S
II-1	Sec-ASD, mus-VSD	Hypoplastic digit (B1)	Normal	Hypoplastic scapula (B)			S	M
II-2	Complete AV canal, multiple mus-VSDs	Absent digit (L1), hypoplastic digit (R1)	Radial deviation	Hypoplastic chest wall, abnormal shoulder girdle			S	M
K3:								
II-1	ASD	Ulnar deviation of distal phalanx (B1)	Normal	Abnormal shoulder girdle		100-101insG	M	M
K4:								
I-2	ASD	Normal	Hypoplastic radius (L)	Hypoplastic chest wall		Trp121Gly	M	M
II-1	ASD	Normal	Hypoplastic radius (L)	Hypoplastic chest wall, narrow shoulders			M	M
III-2	ASD	Hypoplastic digit (L1)	Hypoplastic radius (L), fused radial-ulnar joint (L)	Narrow shoulders			M	M
III-3	ND	Normal	Hypoplastic radius (L)	Hypoplastic chest wall			M	M
IV-1	ASD, 4 mus-VSDs	Clinodactyly (B5)	Normal	Hypoplastic chest wall			S	M
K5:								
II-1	Normal echo and ECG	Triphalangeal thumb (L), hypoplastic digit (R1)	Limited supination of forearm (B)			Thr223Met	M	M
III-1	Sec-ASD, multiple mus-VSDs	Triphalangeal thumb (L)	Normal				S	M
III-2	ASD, multiple mus-VSDs	Triphalangeal thumb (B)	Hypoplastic radius (B)				S	M
K6:								
II-3	ASD, memb-VSD	Absent digit (B1)	Hypoplastic radius (B)			798delA	S	M
K7:								
II-1	PFO, asymmetrical aortic valve	Hypoplastic digit 1 (B), absent scaphoid	Normal	Abdominal <i>situs inversus</i> , vertebral defects (C <sub>2</sub> C <sub>3</sub> and C <sub>6</sub> C <sub>7</sub> fusion)		Gly195Ala	M	M
K8:								
II-1	Sec-ASD, multiple mus-VSDs	Hypoplastic, triphalangeal thumb (B)	Hypoplastic radius (L)			Arg279Ter	S	M
K9:								
II-3	VSD	Triphalangeal thumb (R)	Absent radius (L), hypoplastic ulna (L)			Ser196Ter	M	S
K10:								
II-4	AV canal, memb-VSD	Hypoplastic digit (L1), absent digit (R1)	Hypoplastic radius (B)			Arg237Trp	S	M
K11:								

II-2	PFO, normal ECG	Hypoplastic thenar eminence (L)	Normal	Hypoplastic chest wall	Arg237Gln	M	M
III-1	Sec-ASD	Hypoplastic thenar eminence (L) triphalangeal thumb (B)	Normal	Hypoplastic chest wall		M	M
III-2	Sec-ASD	Absent digit (L1, L2, R1)	Hypoplastic humerus, radius, ulna (B)			M	S
K12:							
I-2	Normal echo	Normal	Normal		Thr223Met	M	M
II-2	Sec-ASD, multiple mus-VSDs	Syndactyly (B1 and 2)	Hypoplastic radius (B)	Abnormal shoulder girdle musculature		S	M
II-3	Multiple mus-VSDs	Syndactyly (B1 and 2)	Hypoplastic radius (B)			S	M
II-5	VSD	Normal	Normal			M	M
K13:							
I-1	Normal echo	Hypoplastic digit (L1)	Normal		Arg237Trp	M	M
II-2	Sec-ASD	Hypoplastic digit (L1)	Limited supination of forearm (L)			M	M
K14:							
II-1	Normal	Hypoplastic distal phalanges	Normal	Cleft palate, facial asymmetry, micrognathia, hypoplastic nails	Ser261Cys	M	M
III-3	Double outlet right ventricle, AV canal	Absent digit (L2)	Hypoplastic radius (L)			S	M
III-4	Normal echo	Hypoplastic distal phalanges (B1-5)	Normal			M	M
K15:							
II-2	VSD	Unknown	Unknown		400-401insC	M	ND
III-1	VSD	Absent digit (B1)	Hypoplastic radius (R)			M	M
III-2	ASD or VSD	Digitalized thumb (B)	Hypoplastic radius (R)			M	M
IV-1	ASD	Digitalized thumb (B)	Normal			M	M
IV-2	Multiple VSDs	Hypoplastic digit (L1), triphalangeal thumb (R)	Normal			S	M
K16:							
II-1	ASD or VSD	Hypoplastic digit (1)	Radio-ulnar synostosis		426-427insC	M	M
III-3	VSD	Absent digit (B1)	Absent ulna and radius (L), hypoplastic humerus (L), hypoplastic ulna and radius (R)			M	S
IV-1	Sec-ASD, 2 mus-VSDs	Absent digit (L1), hypoplastic digit (R1)	Hypoplastic radius (L)			S	M
IV-2	Mus-VSD	Extra digit (R1), triphalangeal thumb (L)	Normal			M	M
K17:							
II-5	Sec-ASD, memb-VSD, mus-VSDs	Hypoplastic metacarpal (B1), hypoplastic digit (L1), triphalangeal thumb (R)	Hypoplastic radius (B)		Thr223Met	S	M
SALL4:							
K18:							
I-2	Normal	Normal	Normal		V752M	M	M
II-1	Truncus arteriosus	Absent digit (L1), hypoplastic digit (R1)	Absent radius (L), hypoplastic radius (R)			S	S
K19:							
I-2	Normal, murmur in childhood	Absent digit (L1), digitalized thumb (R), syndactyly (L2 and 3)	Absent radius (B)	Pelvic kidneys	614-615insCCGT	M	S
II-2	Mus-VSD	Absent digit (L1), digitalized thumb (R)	Absent radius (L)	Hydronephrosis (B), imperforate anus, Duane's anomaly		M	S

<sup>a</sup> ND = no data; echo = echocardiogram; ECG = electrocardiogram; B = bilateral; L = left; R = right; PFO = patent foramen ovale; mus-VSD = muscular VSD; memb-VSD = membranous VSD; sec-ASD = secundum ASD; normal = normal physical examination. Digits are numbered 1-5; from anterior (thumb) to posterior.

<sup>b</sup> M = mild; S = severe; ND = no data.

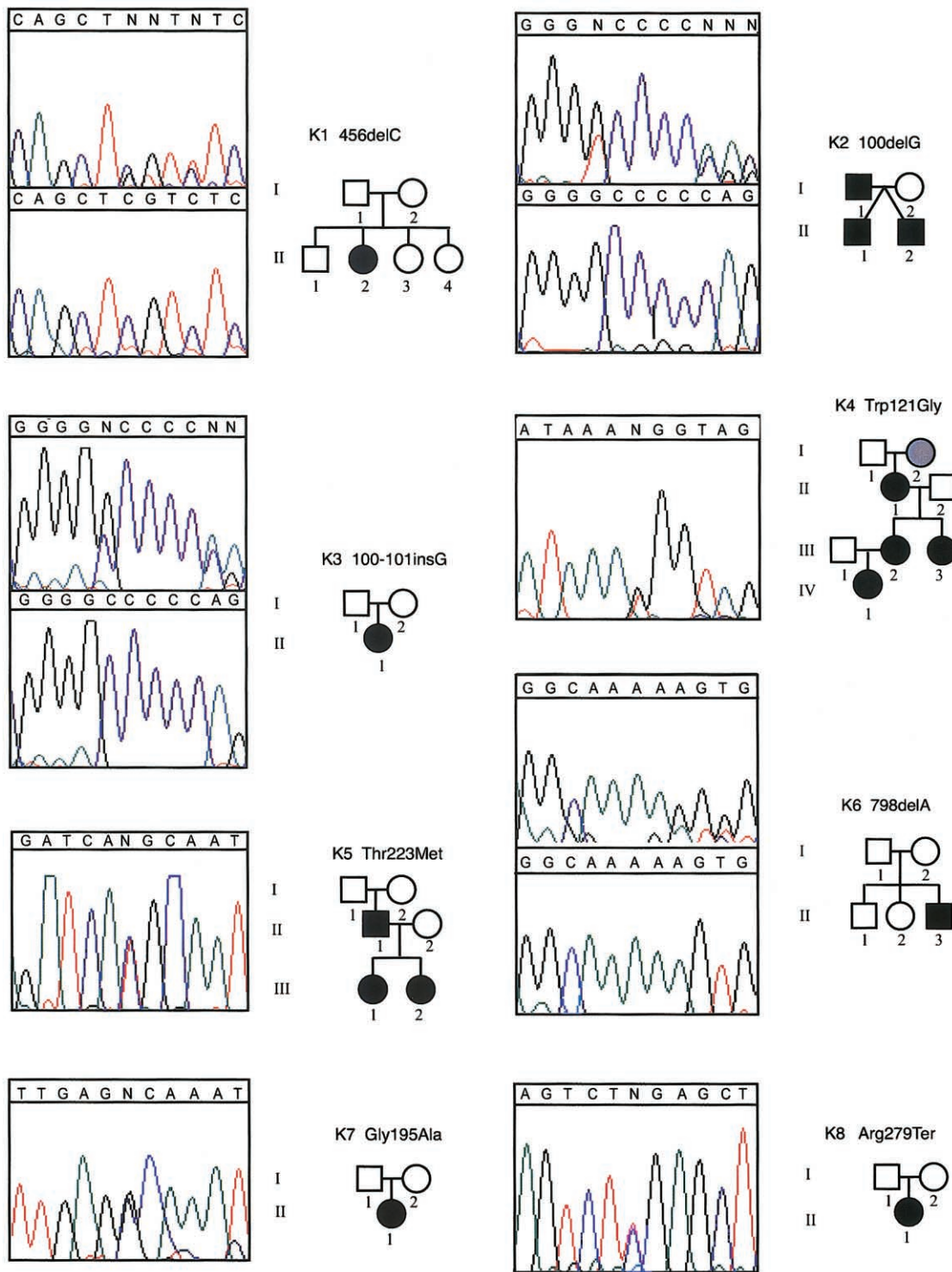
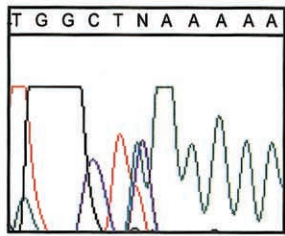
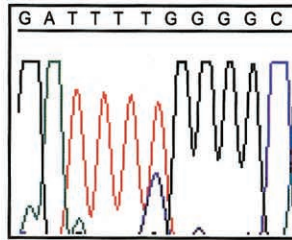
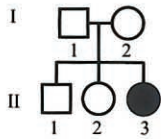


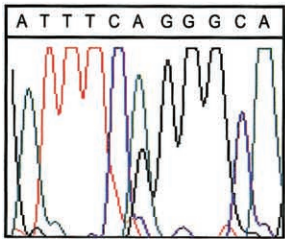
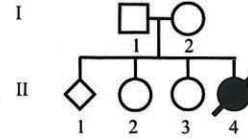
**Figure 1** Pedigrees and electropherograms of 17 families with HOS in which mutations in *TBX5* were found. Affected individuals are denoted by a blackened symbol, unaffected individuals by an unblackened symbol, and unknown phenotypes by a symbol filled with gray. Numbers below each symbol correspond to the identification numbers in table 1, which is a detailed summary of the clinical findings of each affected individual. For frameshift mutations, the mutant and wild-type DNA sequences are shown in the top and bottom boxes, respectively.



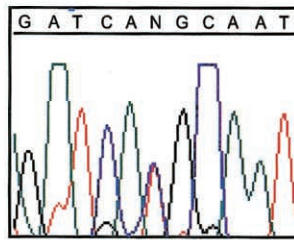
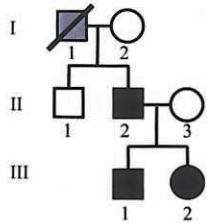
K9 Ser196Ter



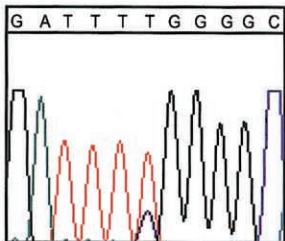
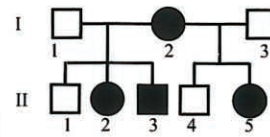
K10 Arg237Trp



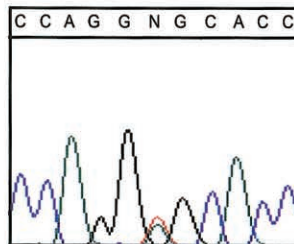
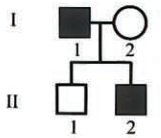
K11 Arg237Gln



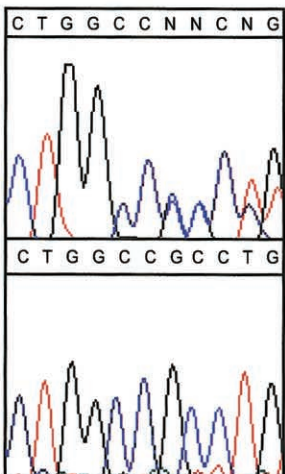
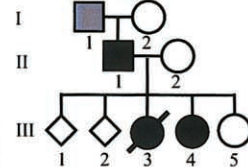
K12 Thr223Met



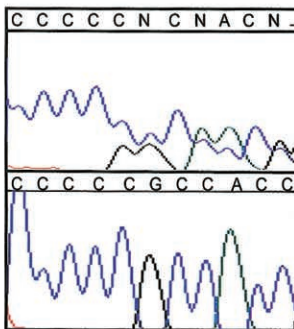
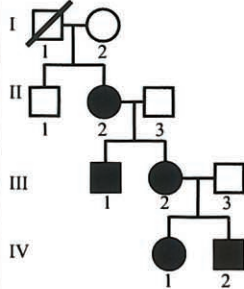
K13 Arg237Trp



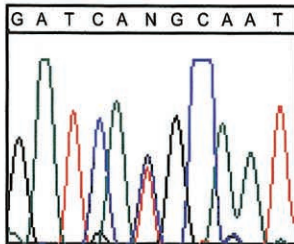
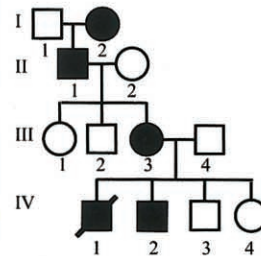
K14 Ser261Cys



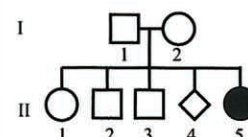
K15 400-401insC



K16 426-427insC



K17 Thr223Met



striction digestion, performed according to manufacturers' instructions, or hybridization to an allele-specific oligonucleotide (see table A [online only]). For each mutation, 150 chromosomes from unrelated, unaffected individuals from a matched ethnic background were also screened. Small deletions and insertions were assessed in at least one affected individual in each kindred by transforming DH5a cells (Invitrogen) with a ligation mixture containing the PCR-amplified product and pCR2.1 plasmid (Invitrogen TA cloning kit). Plasmid DNA was extracted from 10 transformed clones through use of QIA-GEN miniprep columns and was subjected to direct sequencing as described above.

## Results

Fourteen different mutations in *TBX5* were found in 17 (35%) of 49 probands with putative diagnoses of HOS, and 12 of these mutations were novel (fig. 1). Either of two mutations (Thr223Met and Arg237Trp) was found in five unrelated kindreds with HOS. Mutations were detected in 9 of 17 familial cases (53%) of HOS, whereas we were able to identify a mutation in *TBX5* in only 8 of 32 sporadic cases (25%). Thus, the rate of detection in familial cases was approximately twice that in sporadic cases.

Six of the mutations found in *TBX5* are predicted to encode a product that, if translated, would be prematurely truncated prior to or within the T box (fig. 2). This includes one nonsense mutation (Ser196Ter) and five frameshift mutations (100-101insG, 100delG, 400-401insC, 426-427insC, and 456delC). Since deletion of even the most C-terminal amino acid residues of the T box results in loss of *TBX5* binding to its consensus binding sequence in vitro (Ghosh et al. 2001), these mutations likely represent null alleles. A partial *TBX5* protein that includes the T box could be produced in the presence of either of two mutations, 798delA and Arg279Ter. However, both proteins would still lack much of the C-terminal domain of *TBX5*. The mechanism(s) by which 798delA and Arg279Ter disrupt the function of *TBX5* is unclear, because deletion of the entire C-terminal region (amino acids 238–518 inclusive) enhances DNA binding affinity, whereas deletion of amino acids 242 onwards results in loss of binding to the T-binding element (Ghosh et al. 2001).

Six of the mutations found in *TBX5* were missense mutations, four of which have not been reported previously. Each of these mutations is predicted to result in substitution of an amino acid residue of *TBX5* that is highly conserved among species (fig. 3). Five of these amino acid residues are located within the DNA-binding domain of *TBX5*. One predicted amino acid substitution (Ser261Cys) is in the C-terminal domain of *TBX5*, farther downstream of the T box than any missense mu-

tation reported previously. One mutation—Thr223Met, caused by a missense mutation of a CG doublet—was found in three unrelated kindreds, suggesting that this may be a mutational hotspot. Overall, missense mutations were found in ~50% of the probands in whom mutations were identified.

Most individuals in whom a mutation in *TBX5* was discovered had a phenotype typical of HOS, although a wide spectrum of limb and heart malformations was found both within and between families. A total of 16 individuals had mutations predicted to cause truncation of *TBX5* and, in turn, heart and limb malformations of similar severity. Although 6 of these individuals had both mild heart and mild limb defects, 10 individuals had either more severe heart ( $n = 6$ ) or more severe limb ( $n = 4$ ) defects. Moreover, the categorization of phenotypes frequently varied, even within the same kindred. For example, individual I-1 in kindred K2 (fig. 1) has hypoplasia of the left humerus, radius, and ulna and absence of the thumb bilaterally (i.e., severe limb defects) without an accompanying heart defect. In contrast, each of his two sons (II-1 and II-2) have multiple septal defects (i.e., severe heart defects) and unilateral or bilateral hypoplasia/aplasia of the thumb (i.e., mild limb defects).

Twenty-three individuals had missense mutations in *TBX5*. A Trp121Gly substitution in the N-terminal region of the DNA-binding domain of *TBX5* was found in five members of a single kindred. This mutation is predicted to cause severe heart and mild limb defects, and, although each individual had mild limb malformations, only one had a severe heart defect (an ASD and multiple VSDs in individual IV-1). The other four affected individuals had either a single ASD or no detectable structural defect. Fourteen individuals had missense mutations in the C-terminal region of the DNA-binding domain of *TBX5* that were predicted to cause severe limb anomalies and mild cardiac defects. Eight of these individuals, from three kindreds, had a Thr223Met substitution. In contrast to the anticipated phenotype, all eight individuals had mild limb defects, and five of them had severe heart malformations. Six individuals had substitutions of amino acid residue 237, only one of whom had a severe limb anomaly, and two of these individuals with an Arg237Trp substitution had severe heart defects. Overall, 8 of 20 individuals with a missense mutation causing HOS had heart and limb defects of disparate severity. Only 2 of the 20 affected individuals had a pattern of limb and heart malformations consistent with the prediction that mutations in the carboxy- and amino-terminal regions of the T box cause more severe limb and heart malformations, respectively.

The mechanism by which missense mutations in *TBX5* cause HOS remains unclear. We found five different missense mutations in *TBX5* that are predicted to



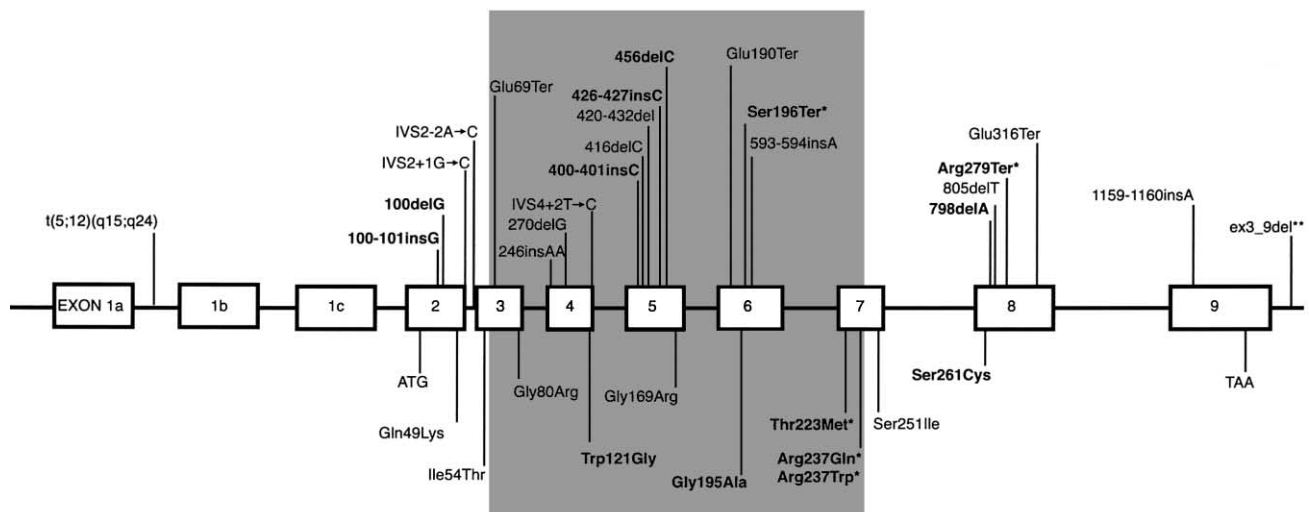


**Figure 2** Schematic of genomic structure of *TBX5* (not drawn to scale), indicating the locations of mutations identified to date. The exons encoding the T box are shaded, and each of the mutations reported in this study is in boldface type. Asterisks (\*) denote mutations that have been found in more than one proband.

cause an amino acid substitution in the T box (Trp121Gly, Gly195Ala, Thr223Met, Arg237Gln, and Arg237Trp). To gain further insight into the effect of these mutations on the function of *TBX5*, we compared the predicted structure of *TBX5* mutants to wild-type *TBX5* by creating a model of the DNA-binding domain of *TBX5* based on the crystal structure of *TBX3* (Coll et al. 2002). The justification for using *TBX3* as a starting point is based, in part, on the observation that the T-box domains of human *TBX3* and *TBX5* share 62% amino acid identity.

The core of the T box consists of a seven-stranded  $\beta$  barrel, which is closed by a lid structure comprising a two-stranded  $\beta$  sheet (fig. 4). The protein contacts the DNA through amino acids located in loops and strands in the lid and from residues in two perpendicular C-terminal helices,  $\alpha$  helix 3 and helix 3<sub>10</sub>C. *TBX5* residue Trp121 corresponds to *TBX3* residue Trp170 in the lid structure where it packs against the core  $\beta$  barrel (“A” in fig. 4). The Trp121Gly substitution in *TBX5* is predicted to destabilize the lid structure, which would likely alter the folding or stability of *TBX5* and disrupt protein-DNA interactions.

*TBX5* residue Thr223 corresponds to residue Thr270 in *TBX3* (“B” in fig. 4). Thr270 is in  $\alpha$  helix 3, where the side chain contacts DNA phosphate backbone atoms, and projects into a relatively open environment in the major groove. Helix 3 and the preceding loop (residues 264–268 in *TBX3*) make important contacts in the major groove. Their position is determined, in part, by an important hydrogen bonding network including Glu229 (Glu180 in *TBX3*), which bridges between

the core  $\beta$  barrel and the loop preceding helix 3 (“C” in fig. 4). Thus, substitution of residue Thr270 or Trp170 is expected to influence DNA recognition residues that normally contact the major groove. Thr270 occupies only part of a small void between the protein and the major groove. Modeling predicts that this space can accommodate a methionine side chain, suggesting that alteration in the activity of *TBX5* does not result from steric clashes between a bulky side chain and DNA.

Arg237Gln and Arg237Trp, corresponding to Arg284 in *TBX3* (“D” in fig. 4), are predicted to disrupt the position and stability of the C-terminal  $\alpha$  helix, (equivalent to  $\alpha$  helix 3<sub>10</sub>C in *TBX3* and  $\alpha$  helix 4 in *Xbra*), thereby affecting binding of *TBX5* to the minor groove of the DNA target (Basson et al. 1999). Gly195 is analogous to Lys242 in *TBX3*. Lys242 is located within a short  $\alpha$  helix that is not present in the *Xbra* crystal structure of the DNA-binding domain of *TBX3* (Muller and Herrmann 1997). This helix is on the surface of the core region distal to the DNA-binding residues and is positioned next to a stretch of four amino acid residues predicted to make weak interactions with a second *TBX3* monomer in complex with the palindromic binding site. Since the function of this part of the protein has not been established, we cannot predict the impact of the Gly195Ala substitution in *TBX5*. One missense mutation in *TBX5* (Ser261Cys) is downstream of the T box. A predicted function of this region of *TBX5* is to interact with modifier proteins (Ghosh et al. 2001). Consequently, this substitution might, if translated into a stable protein, alter the interaction of *TBX5* with a cofactor.



Human	RELWLKFHEVGTETIITKAGRRMFPSYKVKVTGLNPKTKYILLMDIVPADDHRYKFDANR
mouse	RELWLKFHEVGTETIITKAGRRMFPSYKVKVTGLNPKTKYILLMDIVPADDHRYKFDANR
chick	RELWLKFHEVGTETIITKAGRRMFPSYKVKVTGLNPKTKYILLMDIVPADDHRYKFDANR
Zebrafish	RELWTKFHEVGTETIITKAGRRMFPSEKVKVTGLNPKTKYILLMDVVPADDHRYKFDANR
Human	WSVTGKAEPAMPGRLYVHPDSPATGAHWMRQLVSFQKLLKLTNNHLDPFGHIILNSMHKYQ
mouse	WSVTGKAEPAMPGRLYVHPDSPATGAHWMRQLVSFQKLLKLTNNHLDPFGHIILNSMHKYQ
chick	WSVTGKAEPAMPGRLYVHPDSPATGAHWMRQLVSFQKLLKLTNNHLDPFGHIILNSMHKYQ
Zebrafish	WSVTGKAEPAMPGRLYVHPDSPATGAHWMRQLVSFQKLLKLTNNHLDPFGHIILNSMHKYQ
	<b>W121G</b>
Human	PRLHIVKADENNGFGSKNTAFCTHVFPETAFIAVTSYQNHKITQLKIENNPFAKGFGRGSD
mouse	PRLHIVKADENNGFGSKNTAFCTHVFPETAFIAVTSYQNHKITQLKIENNPFAKGFGRGSD
chick	PRLHIVKADENNGFGSKNTAFCTHVFPETAFIAVTSYQNHKITQLKIENNPFAKGFGRGSD
Zebrafish	PRIHIVKADENNGFGSKNTAFCTHVFPETAFIAVTSYQNHKITQLKIENNPFAKGFGRGSD
	<b>G195A</b> <b>T223M</b> <b>R237Q</b>
	<b>R237Y</b>
Human	DMELHRMSRMQ-SKEYPVVPRSTVVRQKVASNHSPFSSESRALSTSSNLGSQYQCENGVS
mouse	DLELHRMSRMQ-SKEYPVVPRSTVVRHKVTSNHSPFSSETRALSTSSNLGSQYQCENGVS
chick	DMELHRMSRMQ-SKEYPVVPRSTVVRQKVSNNHSPFSGETRVLSTSSNLGSQYQCENGVS
Zebrafish	DMELHRMSRMQSTKEYPVVPRSTVVRQKRVGSSQSPFSGDVQGLSATGAISSQYSCENS
	<b>S261C</b>

**Figure 3** Deduced amino acid sequence of partial TBX5 protein in the human, mouse, chicken, and zebrafish. The conserved T-box region is shaded. Missense mutations are indicated in boldface type.

Two individuals with mutations in *TBX5* had findings atypical of HOS: abdominal *situs inversus* in one individual (II-1 in kindred K7), and cleft palate, micrognathia, and facial asymmetry in another (III-3 in kindred K14). These facial abnormalities are, in particular, uncommon in HOS (Allanson and Newbury-Ecob 2003). Interestingly, in the latter case, HOS was caused by a Ser261Cys substitution downstream of the DNA-binding domain of *TBX5*, in a region whose function is unknown. However, other affected individuals in kindred K14 also had atypical findings, such as hypoplastic distal phalanges and fingernails, and a sib without a mutation in *TBX5* had thin hair and hypoplastic teeth. Thus, it is possible that two etiologically distinct disorders are segregating in this family.

Of the remaining 32 kindreds in which mutations in the noncoding and coding regions of *TBX5* were not found, haplotype analysis could not exclude *TBX5*, and no pedigree provided enough statistical power to independently establish linkage to another locus. Some of the affected individuals in these kindreds had defects that are uncommon in HOS (e.g., imperforate anus and truncus arteriosus), suggesting that the etiology of heart and limb malformations in our cohort might be heterogeneous.

Fanconi anemia and Okihiro syndrome (MIM 607323) can be challenging to distinguish from HOS. Okihiro syndrome is thought to be distinguished from HOS by the presence of Duane anomaly, which includes an external ophthalmoplegia. However, Duane anomaly

has a variable age of presentation and can be difficult to detect in the absence of a complete ophthalmological exam. Because Okihiro syndrome has recently been found to be caused by mutations in *SALL4* (Kohlhase et al. 2002), we screened the four exons of *SALL4* in 29 of the remaining kindreds with HOS and discovered two novel mutations (see fig. A [online only]). One mutation, in an individual with sporadic disease, was a G→A missense mutation that causes a Val752Met substitution. This mutation was not found on 230 control chromosomes. However, one parent had the same mutation, but no phenotypic information about this parent was available. Therefore, it is unclear whether this variant is the definitive cause of HOS in this individual. The other mutation identified was a 4-bp insertion that causes a frameshift in *SALL4* in a mother and her son. Only one of these three individuals with a mutation in *SALL4* had an ophthalmoplegia.

## Discussion

When our results are included, a total of 35 different mutations in *TBX5* have been found to cause HOS (Basson et al. 1997, 1999; Li et al. 1997; Cross et al. 2000; Yang et al. 2000; Akrami et al. 2001; Huang 2002). These include missense, nonsense, frameshift, and splice-site mutations; a deletion encompassing exons 3–9 (Akrami et al. 2001); and a translocation that putatively disrupts *TBX5* (Basson et al. 1997). The Arg279Ter mutation, found in a total of six familial and sporadic cases

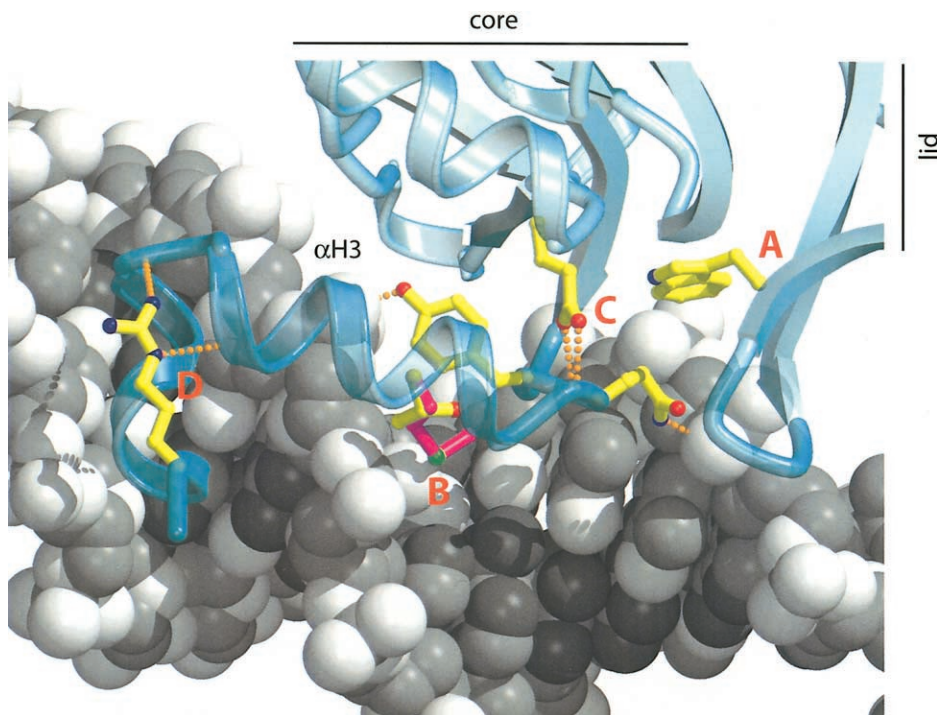


**Figure 4** Ribbon diagram of TBX3/TBX5, shown in turquoise, interacting with DNA, shown as a space-filling model in shades of gray. Important side chains are shown as ball-and-stick models, colored by atom type. Hydrogen bond interactions are shown as dashed orange lines. Perturbations of TBX5 introduced by missense mutations are indicated by A, B, C, and D (see text for details). The TBX5 model is based on the crystal structure of TBX3 from Swiss Prot deep view (Coll et al. 2002). Atomic coordinates for the structure of a TBX3-DNA complex (Protein Database entry 1H6F) were used to create a homology model of TBX5 in complex with DNA. Model manipulations, including changes to the identity and positions of amino acid side chains and examination of hydrogen-bonding networks, were performed with the molecular graphics program O (Jones et al. 1991). Mutations were modeled by changing the relevant amino acid side chains and exploring standard side chain rotamer positions for steric clashes. Atomic figures were generated with the programs MOLSCRIPT (Kraulis 1991) and Raster3D (Merritt and Murphy 1994; Merritt and Bacon 1997).

of HOS, is caused by a C→T transition at bp 1500 that is part of a CG doublet. Accordingly, this site may represent a mutation hotspot in *TBX5*. Three missense mutations (Thr223Met, Arg237Gln, and Arg237Trp) and two nonsense mutations (Ser196Ter and Arg279Ter) account for ~50% of all mutations found thus far in *TBX5*.

*TBX5* mutations were found in only ~30%–35% of sporadic and familial cases meeting the diagnostic criteria for HOS. This is similar to the summarized results of previous surveys of patients who have received diagnoses of HOS (Cross et al. 2000). There are several possible explanations for the low detection rate of mutations. First, some individuals with diagnoses of HOS might be phenocopies, particularly because sporadic heart and limb defects are common, and many of the putative HOS pedigrees were uninformative for linkage analysis. This is supported by the higher mutation detection rate in familial compared with sporadic cases in our cohort. Second, in most studies, only the coding regions of *TBX5* have been screened for mutations. Thus, large deletions or mutations in noncoding regions

that might disrupt the expression of *TBX5* function would not be detected. However, a search for large deletions in 20 cases of HOS in which no mutations in *TBX5* had been found yielded only one new mutation (Akrami et al. 2001). Similarly, screening the UTRs of *TBX5* did not increase our detection rate. Third, HOS may be a genetically heterogeneous disorder. This is consistent with the observation that HOS does not map to 12q24 in some pedigrees (Terrett et al. 1994), although no additional loci have been identified. Finally, there may be regulatory regions important for normal *TBX5* expression that have yet to be identified and that may harbor mutations causing HOS. None of these explanations are mutually exclusive, and each may, in part, be responsible for the low rate of detection of mutations in *TBX5*.

We found no evidence that either the type of mutation or the location of a mutation in *TBX5* was predictive of the severity of limb or heart malformations in an individual with HOS. Most individuals with mutations predicted to truncate *TBX5* did not exhibit heart and

limb defects of similar severity. Moreover, the position of an amino acid substitution in the DNA-binding domain of TBX5 was not predictive of the severity of either the heart or the limb malformations. This result is, however, dependent on the definition of a mild versus a severe malformation. Although we used the classification of Basson et al. (1999) to score severity, the biological justification of this scheme is unclear. For example, it may not be meaningful, in either a clinical or developmental context, to consider absence of the hand and forearm as a mild limb defect while hypoplasia of the thumb, radius, and humerus is considered a severe malformation. Unfortunately, any such dichotomization of limb and heart defects is arbitrary, and, if we reanalyze the HOS phenotypes in our cohort by classifying each malformation separately (e.g., ASD, VSD, triphalangeal thumb, or hypoplastic thumb), *TBX5* genotypes are still not predictive of the type of heart or limb malformation.

An accurate estimate of genotype-phenotype relationships in HOS would be a powerful resource for further exploring the molecular and developmental mechanisms underlying normal cardiac and limb development and for improving the clinical care for patients with HOS. However, this is a challenging objective for any rare malformation syndrome, including HOS. This is due, in part, to the small number of independent cases available for statistical analysis. The size of the sample often is limited further because rare malformation syndromes typically are caused by many different mutations. Inferences about genotype-phenotype relationships for such conditions could be corroborated by data from model organisms. Yet, even highly inbred strains of model organisms with disruptions of genes that cause human malformation syndromes (e.g., see Bruneau et al. 2001) often exhibit widely variable phenotypes. This underscores the substantial degree of environmental and/or stochastic variation that influences the expressivity of many malformation syndromes.

## Acknowledgments

We would like to thank the families for their participation, generosity, and patience, and all of the clinicians who referred study subjects to us. We would like to thank C. T. Basson, J. C. Carey, J. Kohlhase, and R. Newbury-Ecob, for discussion, review, and comments, and L. Rasley and S. W. Watkins, for technical assistance. This project was completed with the support of the Shriners Hospitals for Children, the Primary Children's Medical Center Foundation, the Clinical Genetics Research Program at the University of Utah, the Genomics Core Facility, and the General Clinical Research Center at the University of Utah (grant PHS MO1-00064).

## Electronic-Database Information

The URL for data presented herein is as follows:

Online Mendelian Inheritance in Man (OMIM), <http://www.ncbi.nlm.nih.gov/Omim/> (for HOS and Okhiro syndrome)

## References

- Akrami SM, Winter RM, Brook JD, Armour JA (2001) Detection of a large *TBX5* deletion in a family with Holt-Oram syndrome. *J Med Genet* 38:E44
- Allanson JE, Newbury-Ecob RA (2003) Holt-Oram syndrome: is there a "face?" *Am J Med Genet* 118:314–318
- Bamshad M, Lin RC, Law DJ, Watkins WC, Krakowiak PA, Moore ME, Franceschini P, Lala R, Holmes LB, Gebuhr TC, Bruneau BG, Schinzel A, Seidman JG, Seidman CE, Jorde LB (1997) Mutations in human *TBX3* alter limb, apocrine and genital development in ulnar-mammary syndrome. *Nat Genet* 16:311–315
- Basson CT, Bachinsky DR, Lin RC, Levi T, Elkins JA, Souls J, Grayzel D, Kroumpouzou E, Traill TA, Leblanc-Straceski J, Renault B, Kucherlapati R, Seidman JG, Seidman CE (1997) Mutations in human *TBX5* cause limb and cardiac malformation in Holt-Oram Syndrome. *Nat Genet* 15:30–35
- Basson CT, Cowley GS, Traill TA, Soloman S, Seidman JG, Seidman CE (1994) The clinical and genetic spectrum of the Holt-Oram syndrome (heart-hand syndrome). *N Engl J Med* 330:885–891
- Basson CT, Huang T, Lin RC, Bachinsky DR, Weremowicz S, Vaglio A, Bruzzone R, Quadrelli R, Lerone M, Romeo G, Silengo M, Pereira A, Krieger J, Mesquita SF, Kamisago M, Morton CC, Pierpont ME, Muller CW, Seidman JG, Seidman CE (1999) Different *TBX5* interactions in heart and limb defined by Holt-Oram syndrome mutations. *Proc Natl Acad Sci USA* 96:2919–2924
- Braybrook C, Doudney K, Marcano AC, Arnason A, Bjornsson A, Patton MA, Goodfellow PJ, Moore GE, Stanier P (2001) The T-box transcription factor gene *TBX22* is mutated in X-linked cleft palate and ankyloglossia. *Nat Genet* 29:107–109
- Bruneau BG, Logan M, Davis N, Levi T, Tabin CJ, Seidman JG, Seidman CE (1999) Chamber-specific cardiac expression of *tbx5* and heart defects in Holt-Oram syndrome. *Dev Biol* 211:100–108
- Bruneau BG, Nemer G, Schmitt JP, Charron F, Robitaille L, Caron S, Conner DA, Gessler M, Nemer M, Seidman CE, Seidman JG (2001) A murine model of Holt-Oram syndrome defines roles of the T-box transcription factor *Tbx5* in cardiogenesis and disease. *Cell* 106:709–721
- Burn J, Brennan P, Little J, Holloway S, Coffey R, Somerville J, Dennis NR, Allan L, Arnold R, Deanfield JE, Godman M, Houston A, Keeton B, Oakley C, Scott O, Silove E, Wilkinson J, Pembrey M, Hunter AS (1998) Recurrence risks in offspring of adults with major heart defects: results from first cohort of British collaborative study. *Lancet* 351:311–316
- Coll M, Seidman JG, Müller CW (2002) Structure of the DNA-bound T-box domain of human *TBX3*, a transcription factor

- responsible for ulnar-mammary syndrome. *Structure* 10:343–356
- Cross SJ, Ching YH, Li QY, Armstrong-Buisseret L, Spranger S, Lyonnet S, Bonnet D, Penttinen M, Jonveaux P, Leheup B, Mortier G, Van Ravenswaaij C, Gardiner CA (2000) The mutation spectrum in Holt-Oram syndrome. *J Med Genet* 37:785–787
- Fan C, Liu M, Want Q (2003) Functional analysis of TBX5 missense mutations associated with Holt-Oram syndrome. *J Biol Chem* 278:8780–8785
- Ghosh TK, Packham EA, Bonser AJ, Robinson TE, Cross SJ, Brook JD (2001) Characterization of the TBX5 binding site and analysis of mutations that cause Holt-Oram syndrome. *Hum Mol Genet* 10:1983–1994
- Guyer B, MacDorman MF, Martin JA, Peters KD, Strobino DM (1998) Annual summary of vital statistics—1997. *Pediatrics* 102:1333–1349
- Hiroi Y, Kudoh S, Monzen K, Ikeda Y, Yazaki Y, Nagai R, Komuro I (2001) Tbx5 associates with Nkx2-5 and synergistically promotes cardiomyocyte differentiation. *Nat Genet* 28:276–280
- Huang T (2002) Current advances in Holt-Oram syndrome. *Curr Opin Pediatr* 14:691–695
- Jones TA, Zou J-Y, Cowan SW, Kjeldgaard M (1991) Improved methods for building protein models in electron density maps and the location of errors in these models. *Acta Crystallogr A* 47:110–119
- Kohlhase J, Heinrich M, Schubert L, Liebers M, Kispert A, Laccone F, Turnpenny P, Winter RM, Reardon W (2002) Okinawa syndrome is caused by SALL4 mutations. *Hum Mol Genet* 11:2979–2987
- Kraulis PJ (1991) MOLSCRIPT: a program to produce both detailed and schematic plots of protein structures. *J Appl Cryst* 24:946–950
- Li QY, Newbury-Ecob RA, Terret JA, Wilson DI, Curtis ARJ, Yi CH, Gebuhr T, Bullen PJ, Robson SC, Strachan T, Bonner D, Lyonnet S, Young ID, Raeburn JA, Bucjler AJ, Law DJ, Brook DJ (1997) Holt-Oram syndrome is caused by mutations in TBX5, a member of the Brachyury (T) gene family. *Nat Genet* 15:21–29
- Loffredo CA (2000) Epidemiology of cardiovascular malformations: prevalence and risk factors. *Am J Med Genet* 97:319–325
- Merritt EA, Bacon DJ (1997) Raster3D photorealistic molecular graphics. *Methods Enzymol* 277:505–524
- Merritt EA, Murphy MEP (1994) Raster3D version 2.0—a program for photorealistic molecular graphics. *Acta Crystallogr D* 50:869–873
- Merscher S, Funke B, Epstein JA, Heyer J, Puech A, Lu MM, Xavier RJ, Demay MB, Russell RG, Factor S, Tokooya K, Jore BS, Lopez M, Pandita RK, Lia M, Carrion D, Xu H, Schorle H, Kobler JB, Scambler P, Wynshaw-Boris A, Skoultschi AI, Morrow BE, Kucherlapati R (2001) TBX1 is responsible for cardiovascular defects in velo-cardio-facial/DiGeorge syndrome. *Cell* 104:619–629
- Muller CW, Herrmann BG (1997) Crystallographic structure of the T domain-DNA complex of the Brachyury transcription factor. *Nature* 389:884–888
- Newbury-Ecob RA, Leanage R, Raeburn JA, Young ID (1996) Holt-Oram syndrome: a clinical genetic study. *J Med Genet* 33:300–307
- Schneider MD, Schwartz RJ (1999) Heart or hand? Unmasking the basis for specific Holt-Oram syndrome phenotypes. *Proc Natl Acad Sci USA* 96:2577–2578
- Sletten LJ, Pierpont ME (1996) Variation in severity of cardiac disease in Holt-Oram syndrome. *Am J Med Genet* 65:128–132
- Terrett JA, Newbury-Ecob R, Cross GS, Fenton I, Raeburn JA, Young ID, Brook JD (1994) Holt-Oram syndrome is a genetically heterogeneous disease with one locus mapping to human chromosome 12q. *Nat Genet* 6:401–404
- Yang J, Hu D, Xia J, Yang Y, Ying B, Hu J, Zhou X (2000) Three novel TBX5 mutations in Chinese patients with Holt-Oram syndrome. *Am J Med Genet* 92:237–240